Artificial Intelligence In Medicine 145 (2023) 102687

Contents lists available at ScienceDirect

Artificial Intelligence In Medicine

journal homepage: www.elsevier.com/locate/artmed

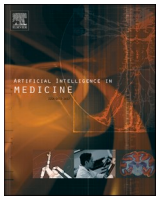

Research paper

Uncovering hidden therapeutic indications through drug repurposing with graph neural networks and heterogeneous data

Adrián Ayuso-Muñoz [a,b], Lucía Prieto-Santamaría [a,b], Esther Ugarte-Carro [a,b], Emilio Serrano [a], Alejandro Rodríguez-González [a,b,*]

[a] ETS Ingenieros Informáticos, Universidad Politécnica de Madrid, 28660 Boadilla del Monte, Madrid, Spain
[b] Centro de Tecnología Biomédica, Universidad Politécnica de Madrid, 28223 Pozuelo de Alarcón, Madrid, Spain

ARTICLE INFO

Keywords:
Drug repurposing
Drug repositioning
Graph deep learning (GDL)
Graph neural networks (GNN)
DISNET knowledge base

ABSTRACT

Drug repurposing has gained the attention of many in the recent years. The practice of repurposing existing drugs for new therapeutic uses helps to simplify the drug discovery process, which in turn reduces the costs and risks that are associated with *de novo* development. Representing biomedical data in the form of a graph is a simple and effective method to depict the underlying structure of the information. Using deep neural networks in combination with this data represents a promising approach to address drug repurposing. This paper presents BEHOR a more comprehensive version of the REDIRECTION model, which was previously presented. Both versions utilize the DISNET biomedical graph as the primary source of information, providing the model with extensive and intricate data to tackle the drug repurposing challenge. This new version's results for the reported metrics in the RepoDB test are 0.9604 for AUROC and 0.9518 for AUPRC. Additionally, a discussion is provided regarding some of the novel predictions to demonstrate the reliability of the model. The authors believe that BEHOR holds promise for generating drug repurposing hypotheses and could greatly benefit the field.

1. Introduction

Drug repurposing or drug repositioning consists in providing novel indications for already existing drugs, using them to treat different diseases from the ones they were originally developed for. By doing so, the drug discovery and development process can be made more efficient, as it can reduce costs, time, and risks associated with drug discovery and development process, what is known as *de novo* approach. Before the development of proper drug repurposing techniques, drug repositioning often occurred serendipitously. However, nowadays, there are many techniques to guide this process, like pathway mapping or genetic association [1].

Observing the scarcity of emergent Deep Learning (DL) techniques among the most common drug repurposing methodologies [1,2] is interesting. Its application, beyond the benefits of drug repurposing itself, could reduce, even further, the cost and time. Drug repurposing with DL has gained popularity in the last years [3–10]. With the increasing trend of conceiving diseases as holistic and interrelated entities [11,12], the use of Graph Deep Learning (GDL) has the potential to make a greater impact due to the large amount of biomedical data available through multi-omics techniques [13–15]. Using GDL it is possible to work directly on graphs, biomedical networks, to gain invaluable insights [16]. The prediction of links between disease and drug pairs in these networks can uncover new indications not considered yet [17].

Previously, following this approach, REDIRECTION (dRug rEpurposing Disnet lInk pREdiCTION) was presented [18]. REDIRECTION is a model trained with part of the DISNET's biomedical graph[1] [19], using a limited set of information: diseases, symptoms, drugs and their relationships. The objective of REDIRECTION was to generate drug repurposing hypotheses by means of link prediction. In this work, BEHOR (Bidirectional Edge and Hyperparameter Optimized Redirection), the model is tested in a richer information set, and contextualized by comparing it against baselines. Some of the top novel drug repurposing hypothesis predictions are studied from a biomedical point of view, to study the reliability of the model's generated hypotheses.

* Corresponding author at: ETS Ingenieros Informáticos, Universidad Politécnica de Madrid, 28660 Boadilla del Monte, Madrid, Spain.
E-mail addresses: adrian.ayuso.munoz@alumnos.upm.es (A. Ayuso-Muñoz), lucia.prieto.santamaria@upm.es (L. Prieto-Santamaría), e.ugarte@alumnos.upm.es (E. Ugarte-Carro), emilio.serrano@upm.es (E. Serrano), alejandro.rg@upm.es (A. Rodríguez-González).

[1] https://disnet.ctb.upm.es/.

https://doi.org/10.1016/j.artmed.2023.102687
Received 8 March 2023; Received in revised form 4 October 2023; Accepted 13 October 2023
Available online 21 October 2023

In addition to the improvements made to REDIRECTION, this work's contribution lies in the use of such a rich and complex set of information for training the model, in terms of the types of relationships it contains. Biological, pharmacological, and phenotypical information is integrated. The model benefits from this rich graph, which provides it with a vast amount of information to help solve the drug repurposing problem. So, drug repurposing benefits from the advantages of using data-driven approaches streamlining the process.

The paper is organised as follows: Section 2 includes a brief revision of how GDL has been used in the context of biomedical data and its uses for drug repurposing. Section 3 details the used datasets, BEHOR's architecture, the training and evaluating process, the used baselines for comparison and the used metrics for evaluation. Section 4 presents the model's results, the evaluation of the selected novel predictions and the limitations. Finally, Section 5 contains the conclusions.

2. Related works

Biomedical information is easily structured as a graph. For example, the Human Disease Network [20], is a graph where the nodes represent diseases and the links between those nodes represent the genetic connections between diseases. Therefore, approaches that can take advantage of the valuable information encoded in this data structure seem promising [21–23]. A graph is a set of items in which there are some pairwise relations, edges. Defined mathematically as it can be seen in Eq. (1).

$$G(V, E), \tag{1}$$

where G is the graph, $V = \{v_1, \ldots, v_n\}$ is the set of vertices, and $E \subseteq \{(v_i, v_j) | v_i, v_j \in V\}$ is the set of edges.

Graphs can be divided into two types, directed and undirected. The directed graphs are the ones in which edges have a direction, whereas the undirected one's edges do not have such condition. So, given an edge $e_i = (v_i, v_j)$, in an undirected graph, this means there is an edge between v_i and v_j, while in a directed graph it means there is an edge from v_i to v_j.

Nodes and edges can be characterized by attributes themselves. For edges, usually, if the value is one-dimensional this is called weight, if not it is called edge attribute. In any case, the representation of an edge would be $e_i = (v_i, v_j, w)$, where w is either the weight or the attribute.

Also, graphs can be divided into homogeneous graphs, graphs where there is just one type of node and one type of edge, and heterogeneous graphs, where there are either multiple types of nodes or multiple types of edges. In the latter case, an edge would be $e_i = (v_i, v_j, r_k)$, where $r_k \in R = \{r_1, \ldots, r_l\}$, being R the set of relation types.

Graphs are such a powerful data structure; their huge expressive capability eases the task of representing diverse types of information. Therefore, DL on graphs could help exploit the latent information available in graphs. Initially, CNN would seem suitable to work with graphs but the incapability of working with non-Euclidean data is a major drawback for its application [24].

Hence, a way of handling graphs in the framework of DL was needed. The precursors of GNN were developed in the late 1990s, applying recursive neural networks to acyclic graphs [15,25,26]. Later, the field of Geometric Deep Learning (GDL) [27] and graph representation learning appeared. The latter's objective is to embed graphs into low dimensionality vectors, which can be accomplished using various algorithms such as DeepWalk [28] and node2vec [29]. But, these algorithms lack of generalization capabilities, they can only generate embeddings for nodes present during the training phase (what is termed transductive setting [15]), resulting in what is called shallow embeddings. Rather than training a model that can generate embeddings for the nodes of a given graph, these algorithms train unique embeddings for every node [30]. Therefore, similar nodes have similar embeddings, and dissimilar nodes have dissimilar ones. Consequently, adding a node to the graph requires training the model again and generating new embeddings.

Thus, GNN and their variations emerged as alternatives with better generalization capabilities [30]. Being able to generate embeddings for unseen nodes, defined as inductive setting. The addition of a new node does not require re-training the model. At the end of the training phase, the result is a function that, given a graph, can generate embeddings for any node in the graph. The use of GNNs for drug repurposing has been successfully demonstrated in previous works [4–7], dating back to 2017 [8], and has yielded promising results. This technique gained widespread attention during the pandemic years when numerous studies focused on repurposing drugs to treat the SARS-CoV-2 virus [31–33].

Some of the first works related to drug repurposing using GDL is Bajaj et al. [8], in which exploration of drug disease interactions is done using a network centred approach. Two types of networks are used: i) PPI with 5489 usable proteins and ii) Disease-Protein interaction network with 534 diseases and their relations with the previous proteins.

Many of the previous works are focused on specific diseases, for example, targeting SARS-CoV-2-virus. In Hsieh et al. [5], the constructed graph contains information related to COVID-19. Similarly, in Zhou et al. [31] two types of human coronaviruses related networks are used in different steps to generate repurposing hypotheses for this disease. The approach measures the interplay between the human coronavirus host interactome and drug targets in the PPI network. In Zeng et al. [32] a massive graph of 15 million edges distributed along 39 types, for 145,179 nodes distributed in 4 node types: drug, gene, disease, and drug side information is used to find drug repurposing candidates for COVID-19. The presented method reported an AUROC of 0.8512.

In addition, centred in COVID-19, but with a generic and adaptable to other diseases, approaches are presented in the following works. In Gysi et al. [4] the used graph contains PPI information, 18,505 proteins and 327,924 interactions between them, interactions between SARS-CoV-2 human proteins and drug-target interactions. In Doshi and Chepuri [6] the used graph is composed by 4 node types and 1,417,624 edges and, for the comparable reported metrics, it presents an AUROC of 0.9240. In the work the authors conduct an analysis of some drug repurposing hypotheses for COVID-19, though it proposes a general method. Moreover, centred in COVID-19 too, in Ioannidis et al. [33] a new method using relational graph convolutional network to solve the link-prediction problem, using this approach drug repurposing hypotheses generation is tackled. Experiments are conducted on the drug repurposing knowledge graph (DRKG) [34], generating repurposing hypotheses for COVID-19. This graph contains 97,238 nodes distributed into 13 types and 5,874,261 edges belonging to 107 edge types.

Changing the focal point, in Sosa et al. [7] the focus is set specifically on rare diseases. The study utilised the Global Network of Biomedical Relationships (GNBR), containing 63,252 nodes and 583,685 edges. It is composed by three node types, drug, disease, and gene. The graph is used to generate drug repurposing hypotheses for rare diseases. It achieves an AUROC of 0.8900.

When it comes to recent works on drug repurposing using GNNs that do not target specific diseases, we find the works of Mei et al. [35] and Gu et al. [36] particularly relevant. In Mei et al. [35] a small graph extracted from the Comparative Toxicogenomics Database (CTD) [37] is used, while applying a two-phase GNN that is composed of a subtype-level network and node-level network encoding modules. In Gu et al. [36], they integrate information from various sources to construct the graph and implement three attention mechanisms into GNNs to address the problem.

Besides drug repurposing, an important work in the field of GDL, the first combination therapy GDL work, is Decagon [38]. Decagon models polypharmacy side-effects using a multi-modal graph containing side effects of drug combinations and protein-protein-interactions (PPI).

We summarise all the cited works in Table 1, where a comparison of the used graph can easily be done. We also include our graph on the last row for comparison purposes.

Table 1
Summary of the Referenced Work's Graphs. Ordered by the nature of the used graph.

Author	Year	Number of nodes (Number of types)	Number of edges (Number of types)	Notes
Zhou et al. [31]	2020	17,706 (1)	351,444 (1)	PPI
Gysi et al. [4]	2021	18,505 (1)	327,924 (1)	PPI
Hsieh et al. [5]	2021	6730 (4)	>5358 (5)	COVID
Zeng et al. [32]	2020	145,179 (5)	15,018,067 (39)	COVID
Doshi and Chepuri [6]	2022	42,484 (4)	1,417,624 (8)	Derived from DRKG
Ioannidis et al. [33]	2020	97,238 (13)	5,874,261 (107)	DRKG [34]
Sosa et al. [7]	2020	63,252 (3)	583,685 (32)	GNBR [39]
Mei et al. [35]	2022	7794 (3)	36,778 (4)	CTD [37]
Gu et al. [36]	2022	41,100 (5)	1,008,258 (10)	Multi-source
Ayuso-Muñoz et al.	2023	153,747 (5)	1,996,658 (12)	–

3. Materials and methods

This section contains the details of the taken approach to carry out the drug-disease repurposing task, the used heterogeneous graphs to train our model, and the GNN related aspects, including the model's architecture, the training, testing, and validating processes, and the RepoDB test.

We have uploaded the materials and results in an accessible repository,[2] so the results can be reproduced.

3.1. Drug-disease link prediction

The drug repurposing problem is formulated as a link prediction task in a heterogeneous graph of diseases and their interactions with various entities, like drugs or proteins. Link prediction is performed between disease and drug node types.

The results of the model can be interpreted as the confidence of the model in the existence of a given link, being zero no confidence and one absolute confidence. Then the problem is solved as a binary classification problem, where the classes are non-existent (0) and existent (1).

3.2. Dataset

The employed data to build the heterogeneous graph, Tables 2 and 3, originates from the DISNET database [19], which is a biomedical integrated knowledge base containing information regarding diseases and their associations to symptoms and drugs, among others. More information about the data typologies, including the sources of the data and date of extraction, are indicated in Table 1 of the Supplementary Material. Note that, node type "*phenotype*" contains both "*disorders*" and "*symptoms*".

Table 2
Number of nodes per node type and its contribution to the total.

Node type	Count	Percent (%)
Phenotype	30,731	19.99
Drug	3944	2.56
Pathway	1105	0.72
Protein	18,521	12.05
DDI	99,446	64.68
Total	153,747	100

Table 3
Number of relations per relation type and its contribution to the total.

Relation type	Count	Percent (%)
Disease-protein	360,985	18.08
Disease-drug (therapeutic)	52,179	2.61
Disease-symptom	318,550	15.96
Disease-pathway	424	0.02
Drug-drug	662,281	33.17
Drug-protein	5946	0.30
Drug-symptom (side effect)	45,516	2.28
Drug-symptom (indication)	863	0.04
Protein-protein	240,585	12.05
Protein-pathway	10,991	0.55
DDI-phenotype	99,446	4.98
DDI-drug	198,892	9.96
Total	1,996,658	100

The node features are initialised as a 100-dimensional vector, values are set to 1 since there are no specific node features and the algorithm needs them for functioning. Other approaches include assigning node identification in binary or randomly generated vectors. In any case, the results would be similar, because none of the options encapsulate true properties of the nodes and the algorithm will modify them accordingly.

To construct a particular evaluation set, the RepoDB test, information from RepoDB [40] is extracted. RepoDB contains a set of drug repositioning successes and failures that can be used to benchmark computational repositioning methods. The RepoDB cases are removed from the graph before entering the model's pipeline. The training, validating, testing, and evaluating sets are disjunct, there is no data leakage between sets.

The choice of a heterogeneous graph is significative, since it is an efficient way of incorporating a great variety of information in the same data structure. This way the information between different types of nodes (phenotypes and drugs) can flow easily, enrichening the underlaying information the model uses to make predictions.

3.2.1. Simple graph

The simple version of the graph used a reduced set of nodes and relations. Node types were "*phenotype*" (30,731) and "*drug*" (3944), resulting in a total of 34,675 nodes. Edge types were "Disease-Drug" (relationships considered to have a therapeutic effect) (52,179), "*dis_dru_the*", and "Disease-Symptom" (318,550), "*dse_sym*", resulting in a total of 370,729 edges. The representation of the schema followed by this graph can be seen in Fig. 1.

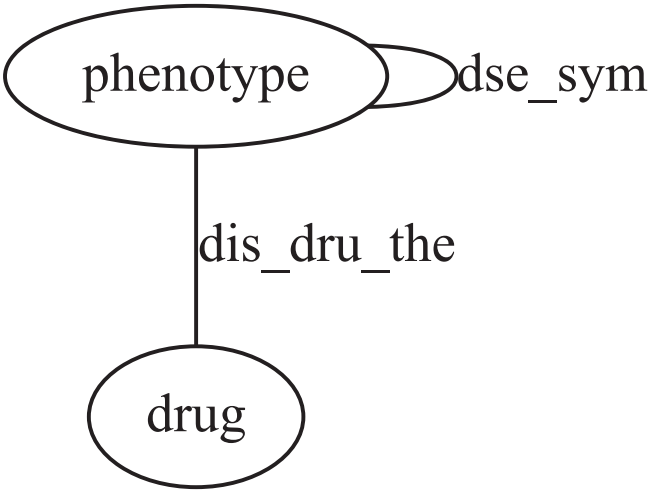

Fig. 1. Schema of the nodes and relations of the simple graph.

[2] https://zenodo.org/record/8402843/files/aiim2023-gnns-master.zip.

3.2.2. Complex graph

This version of the graph uses all the available information. Node types are "*phenotype*" (30,731), "*drug*" (3944), "*pathway*" (1105), "*protein*" (18,521) and "*drug-drug-interaction*" (99,446), in total 153,747 nodes. Edge types are Disease-Drug (therapeutic) (52,179), "*dis_dru_the*", Disease-Symptom (318,550), "*dse_sym*", Disease-Protein (360,985), "*dis_pro*", Disease-Pathway (424), "*dis_pat*", Drug-Drug (662,281), "*druA_druB*", Drug-Protein (5946), "*dru_pro*", Drug-Symptom (side effect) (45,516), "*dru_sym_sef*", Drug-Symptom (indication) (863), "*dru_sym_ind*", Protein-Protein (240,585), "*proA_proB*", Protein-Pathway (10,991), "*pro_pat*", DDI-Phenotype (99,446), "*ddi_phe*", and DDI-Drug (198,892), "*ddi_dru*", in total 1,996,658 edges. A representation of the schema followed by this graph can be seen in Fig. 2.

3.3. Graph neural network

The goal is to predict the probability of an edge existing between a given disease-drug pair. To achieve it, graph information will be used to generate embeddings of the entities by a GNN encoder, and then calculate the edge's probability by means of a simple decoder. The problem is approached as an end-to-end problem, where the encoder and the decoder are optimized in tandem.

3.3.1. Model architecture

The architecture is divided in two different parts, clearly separated. The aim of the model is to solve the link prediction task, but each part of the architecture specializes in a different problem. Encoder generates representations of the nodes, while decoder uses those representations to predict the probability of an edge's existence between two nodes.

Generating node's representative embeddings is the encoder's task. This step is crucial to the final performance of the model. Embeddings must capture all the important features of a node in a graph. The encoder's architecture, depicted in Fig. 3, has two layers. After each of them a batch normalization takes place. Between the layers, there is a leaky rectified linear unit (LReLU), providing non-linearity, and a dropout layer, to reduce variance.

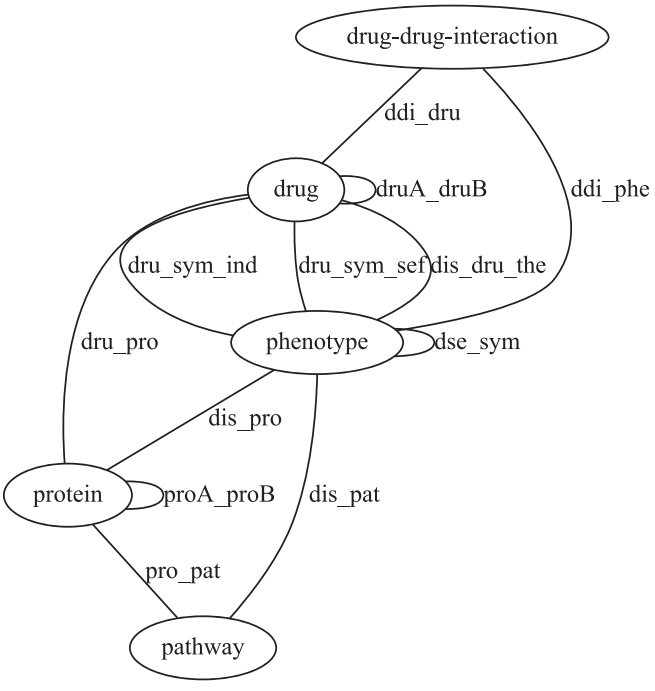

Fig. 2. Schema of the nodes and relations of the complex graph.

Layers use GraphSAGE[3] as a framework [41]. First, a node's neighborhood is sampled; then, the information of the sampled neighbours is aggregated, generating a new embedding for the node, Eq. (2) [41]. This process efficiently generates node embeddings inductively. Since there are two of these layers, the model generates final embeddings using 2-hop neighborhood information.

$$h_v^k = \sigma\left(W^k MEAN\left(\left\{h_v^{k-1}\right\} \cup \left\{h_u^{k-1}, \forall u \in N(v)\right\}\right)\right) \tag{2}$$

where, h_v^k is the embedding of node v at iteration k, W^k the weights matrix of a fully connected layer, $N(v)$ the neighbour sampler function and $\sigma(x)$ the sigmoid function. In this case, $k = \{1, 2\}$, since the 2-hop neighborhood is sampled. Aggregating part is $AGG = \left\{h_u^{k-1}, \forall u \in N(v)\right\}$ and updating is $\sigma\left(W^k MEAN\left(\left\{h_v^{k-1}\right\} \cup AGG\right)\right)$.

Once the embeddings have been generated, the decoder will calculate he probability of an edge existing between a disease and a drug. To compute it, the sigmoid function is applied to the dot product of the embeddings, as seen is Eq. (3).

$$P = \sigma\left(x_{disease} \cdot x_{drug}^T\right) \tag{3}$$

Being $x_{disease}$ the embedding vector of a disease node, x_{drug}^T the transpose of the embedding vector of a drug node and $\sigma(x)$ the sigmoid function.

3.3.2. Training, testing and evaluating

We split the available data into three sets, train, test, and validation sets. To train the model, the specific training set, formed by the 80 % of the data of the original graph is employed. The remaining 20 % of the data is divided as it follows: 10 % is assigned for internal training validation tasks (*i.e.*, to avoid overfitting, to tune the hyperparameters, and to ensure the absence of data leakage) and a 10 % for testing tasks.

Decoder does not require training, there are no parameters, so just the encoder undergoes the training phase. We trained the encoder using the output of the decoder as the predicted value and of an edge existing in the graph as target value.

During the training phase, model's parameters are adjusted using the Binary Cross Entropy with Logit Loss (BCELogitLoss) as the loss function, which is computed as it can be seen in Eq. (4).

$$\begin{aligned} l(x, y) = L = \{l_1, \ldots, l_N\}^T, \\ l_n = -[y_n \bullet log\sigma(x_n) + (1 - y_n) \bullet log(1 - \sigma(x_n))] \end{aligned} \tag{4}$$

where x_n is the model's prediction and y_n the true label (whether the edge exists or not). We perform negative sampling [42,43], that is, for each edge in the graph (positive edge), we sample a random edge (negative edge) that is not present in the original graph. The ratio between positive and negative edges while training is one.

Hyperparameter tuning is conducted using Weight & Biases [44] platform, which automates and eases this process. The hyperparameter space is defined based on experience and intuition gained from previous executions of the model. The hyperparameter optimisation used a Bayesian approach, so it did not explore all the possible combinations. The set of selected hyperparameters is the one with the higher average area under the receiver operating characteristic curve (AUROC) tested on the validation set, estimated through repeated hold-out with $k = 20$. The selected set of hyperparameters is 2752 epochs, 0.0008317 learning rate, 107 hidden dimensions, 0.006314 weight decay and 0.8 dropout.

[3] https://snap.stanford.edu/deepsnap/_modules/deepsnap/hetero_gnn.html#HeteroSAGEConv.

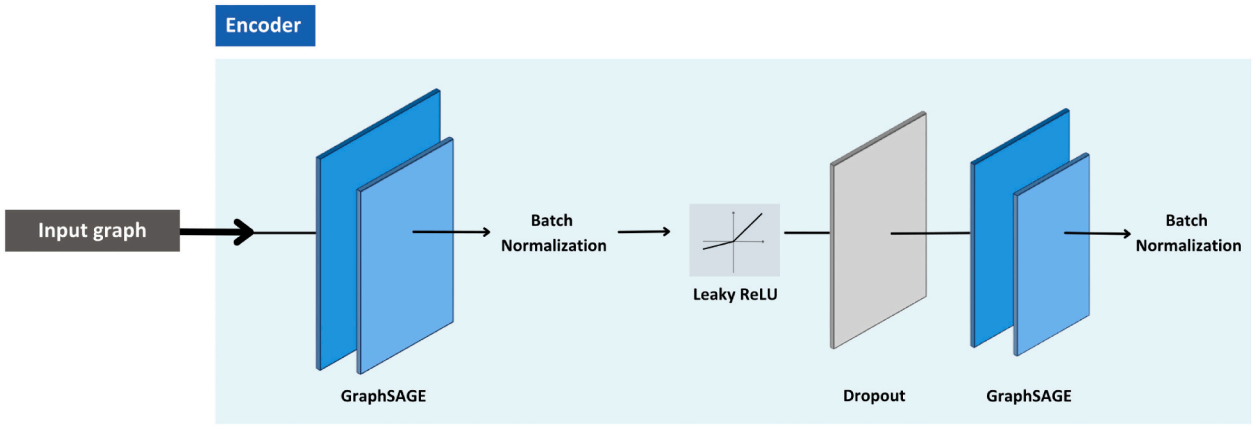

Fig. 3. Structure of the Graph Neural Network encoder. There are two graph convolution layers followed by a batch normalization. In between the convolutions there is a LReLU and a dropout layer.

As a brief analysis of the hyperparameters, the parameter importance with respect to the AUROC, one of the metrics we use. Weight & Biases platform provides this analysis, showing correlation and importance. It uses random forest technique to calculate the importance of each hyperparameter. Weight decay's correlation is −0.767 and importance 0.457, learning rate's correlation is −0.737 and importance 0.313, hidden dimensions' correlation is −0.288 and importance 0.111, epochs' correlation −0.153 and importance 0.051 and dropout's correlation is 0.351 and importance 0.022.

Those results show that weight decay is the most important hyperparameter for the model's performance, and that the higher the weight decay value the lower the reported metric's value. The highest value tested is 0.04745 and the lowest 0.0001422. The rest of the metrics are analysed in an analogous way. As for the learning rate, the highest tested value is 0.06807 and the lowest 0.000106. The highest value tested for the hidden dimensions is 128 and the lowest is 9. The model that was trained for the most epochs was trained for 9529 epochs and the one trained with the fewest epochs was trained for 413 epochs. Dropout analysis is different since its correlation is positive. The higher the dropout value, the better the reported metric's value. The highest tested dropout value is 0.9 and the lowest 0.4.

The interaction between the hyperparameters is complex, the values of correlation and importance we supply are just an indicator of what could be happening inside the model.

3.3.3. *RepoDB test*

To ensure reliability, especially important in this context, we perform a second evaluation with RepoDB [40]. The connections between drug and diseases that RepoDB offers are used to validate and interpret the results returned by the trained predictor.

Among these cases, 5013 repositioning drug-disease pairs are selected, of which 1824 are present in our graph and had to be taken out (1824). As for the nodes, we selected only the cases from RepoDB where both the drug and the disease node were already in the graph. Since the nodes are involved in other relations none of them are taken out. The selected pairs are fed into the trained model, ideally, all pairs should have one as their score value.

Moreover, to guarantee the quality of the model and to supplement this test, another set of 5013 randomly generated drug-disease pairs is fed into the model. In this case, ideally, all pairs should have 0 as their score value, since the probability of picking a valid pair for repurposing is considerably small.

Note that, among the 5013 repositioning pairs from RepoDB there are elements of the four following classes: i) approved, ii) terminated, iii) withdrawn and iv) suspended. Initially, the four classes were treated separately but results were similar, so classes were joined. This was done under the following assumption: if a drug-disease pair was tested this indicates that there is a relevant relation that induced this study. Whether the drug was finally repurposed or not is not as important as identifying that the drug could be potentially repurposed.

This test verifies that the tested models can identify new drug repurposing cases, even though, it cannot be assured if this case will be, finally, approved or not. It is important to note that this process only serves as a preliminary step in identifying which drug repurposing pairs are worth further investigation, with experimental validation being necessary.

3.4. *Experimental setup*

To contextualize the results of BEHOR, it is compared against five baselines for working on graphs:

- DeepWalk [28] uses short fixed length random walks to obtain local information, therefore relying on structural information, independent of label's distribution, to generate the embeddings in an unsupervised way. Random walks are uniformly sampled. It uses SkipGram [45] to fit node representations, since random walks can be seen as a sentences and nodes as words the application of this model is direct. The idea is, given a random walk, to estimate the likelihood of observing a certain node. In other words, to relate each node to its context.
- Node2Vec [29] works quite similarly to DeepWalk, the only difference is how the set of neighbouring nodes and random walks are defined. Here, random walks are not uniformly sampled, this method introduces biased random walks, using probabilities, extrapolating between local and global views. Consequently, diverse neighbourhoods of a node are explored, and richer embeddings are generated.
- NetMF [46] proposes itself as matrix factorization method with closed forms unifying skip-gram models, like DeepWalk or Node2-Vec. It lays its foundations on the basis that all the previously mentioned methods perform implicit matrix factorization. NetMF explicitly factorizes those closed-form matrices.
- Role2Vec [47] generalizes previous random walk methods, such as DeepWalk or Node2Vec. The main difference is that it can be used in inductive and transductive settings and the capability of integrating node's features. Using attributed random walks as its core, it learns functions that generalize to new nodes and graphs. Attributed random walks, in essence, is a random walk that also captures information about node features.
- REDIRECTION [18] is the previous version of the model. There are 2 important changes: i) edges are undirected, which yields an

important performance improvement; and ii) hyperparameter optimization. Moreover, this version was only trained for the simple graph.

DeepWalk, Node2Vec and NetMF baselines are called shallow encoders and produce shallow embeddings. This means, each node has a unique embedding, in fact these methods are called embedding lookup methods [30]. Moreover, these baselines are transductive, embeddings can only be generated for nodes present during training, they lack generalization capabilities, as opposed to Role2Vec, REDIRECTION or BEHOR, inherently inductive. Every model uses a an inner-product decoder. No hyperparameter optimization is done, default hyperparameters are used for every baseline.

To ensure representative results, all the metrics were estimated using multiple resampling-based estimation methods.

The baselines tests were developed in Python 3.8.15, using PyTorch 1.10.2, DGL 0.7.2 and NetworkX 2.6.3. We made use of CUDA Toolkit 11.3, running the experiments on an Ubuntu Server LTS 20.04.4 with a GPU (NVIDIA GeForce RTX 3090 24GB). For testing DeepWalk, Role2Vec, Node2Vec and NetMF baselines Karate Club library [48] was used. All the materials and results related to the baselines testing have been published in an accessible repository,[4] to make the results that have been obtained reproducible.

3.5. Evaluation metrics

To evaluate the models the receiving operating characteristics (ROC) curve and precision-recall (PR) curve are used. The curves are analysed visually, but to ease the comparison between models the area under (AU) each curve is used.

ROC curves were used to asses model performance in 1989 for the first time [49]. These curves are constructed by plotting the true positive rate (TPR) against the false positive rate (FPR) using different thresholds. TPR is the proportion of correctly labelled positive instances out of all the positive instances. FPR is the proportion of wrongly labelled negative instances, labelled as positive, out of all the negative instances. Using the AU, the perfect classifier has a value of 1, while the random one has a value of 0.5. Note that, ROC curves are biased when working with imbalance, they are biased towards the majority class. In this work there is no class imbalance.

PR curves, in this work, are used as a complementary metric to ROC. The use of PR curves is especially interesting in those cases where FPR is small [50]. These curves are constructed by plotting the precision against the recall using different thresholds. Precision is the proportion of correctly labelled positive instances out of all the labelled positive instances. Recall is the same as TPR. The higher the AU, the better, up to one.

In this work, out of the presented metrics, precision will be particularly considered. High precision models will offer a set of predictions with high confidence, all positive instances may not be recovered, but the recovered ones have quite a high prediction of being truly positive.

4. Results and discussion

4.1. Results

All the presented results are obtained using multiple resampling-based estimation methods during training time and reporting the results obtained on the RepoDB test, so there is certain stability of the estimates. Cross validation is generally the best approach to obtain the estimations, but it can be computationally expensive [51]. Due to time complexity and the large dataset, we estimate values through repeated hold-out with $k = 20$.

[4] https://zenodo.org/record/8402843/files/aiim2023-baselines-master.zip.

Confidence intervals (95 %) are calculated using the t-distribution, since the number of samples is under thirty. The number of degrees of freedom is nineteen.

Table 4 contains the comparison of the baselines' results and BEHOR. REDIRECTION was just trained and tested on the simple graph. As observed, the presented models overperform the baselines by a large margin. The model trained on the complex version of the graph performs slightly better than the simple one and its variance is lower, it is overall a better performing and more stable model. Reported metrics show great results for BEHOR models, proving the capacity of them to identify novel therapeutic indications through drug repurposing.

The complex model improves the simple previous model by, approximately, 0.09 for the AUROC and 0.12 for the AUPRC. Although it may not seem like a significant improvement, it is noteworthy considering the impressive results achieved by the previous model.

4.2. Novel predictions

The graph contains over 121 million potential hypotheses for drug repurposing. To narrow down the options for study, a set of filters were applied. The first filter was used to select cases with 1 as a prediction score, reducing the cases to approximately 1.5 million. The second filter further narrowed down the options by selecting diseases with no existing therapeutic treatments in the graph and with a T047 semantic type (disease or syndrome), resulting in a reduction to over 165 thousand cases. The third and final filter, was applied to select those cases containing drugs associated to fewer than 15 diseases in the graph, leaving 4599 cases for study. The decision to set the threshold at 15 was based on the distribution of phenotype-drug associations shown in Fig. 1 of the Supplementary Material.

Once these filters are applied, a series of model generated novel predictions are selected for further analysis, Table 5.

The first discussed hypotheses are the ones for **Congestive Heart Failure**. Congestive heart failure is a severe illness characterized by indications of impaired ventricular function [52]. It may result from several heart diseases and is a significant concern in global health policy [53].

- **Nestiride** is a recombinant human B-type natriuretic peptide (BNP) with advantageous effects on vasodilation, sodium and fluid excretion, and the nervous system [54]. This drug mimics the actions of endogenous natriuretic peptides causing balanced arterial and venous dilatation. Due to the decrease of systemic vascular resistance, systemic arterial pressure, pulmonary capillary pressure, right atrial pressure and mean pulmonary arterial pressure, it is administered intravenously for the management of adult patients with decompensated congestive heart failure [54,55]. In addition, studies

Table 4
AUROC and AUPRC for every baseline and the presented model. The test is conducted on the two graph types, the simple and the complex one. Bold type indicates the best results among the ones seen for each column.

Baseline	Simple		Complex	
	AUROC	AUPRC	AUROC	AUPRC
DeepWalk	0.3842 ± 0.0021	0.4526 ± 0.0015	0.4865 ± 0.0023	0.4831 ± 0.0015
Node2Vec	0.3899 ± 0.0022	0.4567 ± 0.0013	0.4830 ± 0.0022	0.4829 ± 0.0015
NetMF	0.6120 ± 0.0005	0.6463 ± 0.0011	0.7457 ± 0.0013	0.6964 ± 0.0018
Role2Vec	0.6675 ± 0.0012	0.6939 ± 0.0019	0.6735 ± 0.0014	0.6874 ± 0.0019
REDIRECTION	0.8700	0.8300	–	–
BEHOR	**0.9550 ± 0.0017**	**0.9484 ± 0.0019**	**0.9604 ± 0.0006**	**0.9518 ± 0.0009**

Table 5
Top N novel predictions of the model. All the presented hypotheses got the maximum prediction score (1).

Disease UMLS CUI	Disease name	Drug CHEMBL ID	Drug name	Clinical trials
C0018802	Congestive heart failure	CHEMBL1201668	Nesiritide	554
		CHEMBL1351	Liraglutide	23
C0003873	Rheumatoid arthritis	CHEMBL960	Leflunomide	78
		CHEMBL1789941	Ruxolitinib	4
C0149721	Left ventricular hypertrophy	CHEMBL3137301	Sacubitril	8

have shown that Nesiritide is well tolerated in children with heart failure and is associated with improved diuresis [56].

- **Liraglutide** is a synthetic analogue of human glucagon-like peptide-1(GLP-1) and acts as a GLP-1 receptor agonist [57]. It is indicated for weight loss and Type 2 Diabetes Mellitus. This drug rises the levels of cyclic AMP boost insulin release based on glucose levels, block glucagon release based on glucose, and slow down stomach emptying for better blood sugar control [58]. Liraglutide has been demonstrated to have beneficial effects on heart function in patients with Type 2 Diabetes and heart failure improving the left ventricular ejection fraction [59].

The secondly discussed hypotheses are the ones for **Rheumatoid Arthritis**. Rheumatoid Arthritis (RA) is a chronic autoimmune disease characterized by persistent synovitis, systemic inflammation, and autoantibodies (particularly rheumatoid factor and citrullinated peptide) [60]. It is the most common inflammatory arthritis, and a significant cause of morbidity and mortality [61], affecting approximately 0.5–1 % of the worldwide population.

- **Leflunomide** is a disease-modifying anti-rheumatic drug (DMARD) and is actually approved for the treatment of RA [62–64]. Several mechanisms of action of leflunomide have been described, but the main mechanism responsible for its effectiveness in treatment of RA is the ability of A77-1726 to inhibit dihydroorotate dehydrogenase, the rate-limiting enzyme for *de novo* synthesis of pyrimidine nucleotides [65,66]. In autoimmune diseases such as RA, activated lymphocytes require an increased pyrimidine nucleotide pool (at least 8-fold) to progress from G1 to S phase of the cell cycle. Inhibition of pyrimidine synthesis by leflunomide results in decreased pyrimidine nucleotide pools, thereby inducing cell-cycle arrest and inhibition of lymphocyte clonal expansion in patients with RA [67].
- **Ruxolitinib** is a potent and selective oral inhibitor of Janus kinase (JAK) 1 and JAK2 [68]. JAKs are multidomain non-receptor tyrosine kinases that have pivotal roles in cellular signal transduction. Activation and transphosphorylation of JAKs induce signal transducer and activator of transcription (STAT) recruitment, dimerization, nuclear translocation, and resultant transcriptional responses [69]. Therefore, JAK–STAT signalling has a pivotal role in a pleotropic range of systems, including the orchestration and functional capability of immune responses [70,71]. Due to this central role of JAKs in the immune response and their association with several cytokine receptors, the inhibition of JAKs appeared to be a promising strategy in autoimmune diseases [72], including RA. Ruxolitinib is already licensed for the treatment of some myeloproliferative neoplasms (MPNs) and some studies have already pointed out its utility for RA [73–75].

Finally, the hypotheses for **Left Ventricular Hypertrophy**. Left ventricular hypertrophy (LVH) is a cardinal manifestation of end-organ damage due to hypertension; its reported prevalence has ranged from 36 to 41 % in echocardiographic studies in individuals with elevated blood pressure [76]. The development of pathologic LVH is classically attributed to a maladaptive response to long-standing pressure-volume overload of the left ventricle (LV). The cellular hallmarks of hypertensive heart disease (HHD), including cardiomyocyte hypertrophy and fibrotic changes in the non-cardiomyocyte components of myocardium, have implicated a variety of causal factors such as neurohormonal activation and other signalling pathways [77,78].

- **Sacubitril** is usually combined with valsartan as a fixed-dose combination (FDC) to treat several types of heart failures in different conditions [79,80]. Sacubitril/valsartan is the first in a new class of drug: the angiotensin receptor–neprilysin inhibitors (ARNI). Its mechanisms of action have not been well defined. Sacubitril/valsartan causes simultaneous augmentation of the natriuretic peptide system (NPS) and inhibition of the renin–angiotensin–aldosterone system (RAAS) [81]. RAAS inhibition by valsartan has been extensively tested in patients with heart failure (HF) [82]. However, the actions of sacubitril remain unknown.

4.3. Limitations

We are aware the presented work has some limitations. One of the main limitations is the lack of features for the nodes in the graph. Therefore, losing some advantages of the GraphSAGE algorithm and the potential results improvement that could take place if the model made use of that information. Other main limitation we notice is the great difference in the model's predictions depending on the nodes. Nodes that have many connections in the graph will tend to have higher scores than those that are isolated. So, the model is biased towards the nodes with higher connectivity. We plan to address this in the future, some ideas are pruning the graph or the focus on specific information for every node. The same way, because of the way the learning of the model takes place, those nodes that do not have any connections in the graph will not get useful predictions.

The work is limited too in the relationships it can predict, its use cases, the model is just trained to predict Disease-Drug (therapeutic) edges. The rich heterogeneous graph allows holding many relationship types in the same data structure. We could make the model take advantage of all the available information and predict any edge type. Though, for this work, we gave more importance to the specialisation on drug repurposing.

5. Conclusions

The use of heterogeneous biomedical information structured as a graph has proven valuable in combination with GNNs to tackle the drug repurposing problem. Additionally, the generation of drug repurposing hypotheses by BEHOR, framed in the GDL field, has the potential to streamline the drug repurposing process and reduce costs and time. The analysis of some novel predictions generated by BEHOR indicates its ability to produce valid drug repurposing hypotheses, which was further confirmed by the results of testing with both the test graph and the RepoDB test.

The primary contribution of this paper is the development of a GDL model on a complex and rich set of information, DISNET, to train drug repurposing hypotheses. This new model surpasses its predecessor by roughly 0.09 for AUROC and 0.12 for AUPRC in the RepoDB test. While this improvement may appear small, it is significant given the impressive results obtained by the previous model, 0.87 for AUROC and 0.83 for AUPRC. In addition, the discussion of a set of novel predictions validates the potential of this method.

Nonetheless, it should be noted that BEHOR's predictions cannot be considered as a definitive truth and require experts and experimental validation. It is crucial to understand that BEHOR should not be viewed as a substitute for medical prescription systems. Rather, it serves as a tool to suggest potential drug repurposing pairs that may be worth further investigation.

As for the future lines, a number of improvements are possible, such

as the further exploration of the hyperparameter space. However, there is one critical area that needs to be prioritized, which is the incorporation of node features. There are no features for the nodes, GNNs would greatly benefit from the presence of node features. It is expected to gain a great performance improvement with its inclusion, but which features to incorporate is a question that has not been solved yet.

Among the other future research directions, which are of lower priority, it could be interesting to observe the model's behaviour under different circumstances. Testing different types of encoders, such as other types of classic GNNs, other types of decoders, since the used encoder is simple and has no parameters, like the use of multilayer perceptron (MLP) and loss functions could provide valuable insights. Distinguishing between the different RepoDB classes is also an intriguing avenue for future research. Finally, the development of more sophisticated evaluation techniques is an interesting direction for future work. The RepoDB test verifies that the tested models can identify new drug repurposing cases, even though, it cannot be assured if this case will be, finally, approved or not.

Data and code availability

The data employed and code developed for the present study are openly available at https://zenodo.org/record/8402843.

Zenodo repository is a clone with the content, also available in GitLab, of the following repositories:

https://medal.ctb.upm.es/internal/gitlab/disnet/gnns/aiim2023-gnns

https://medal.ctb.upm.es/internal/gitlab/disnet/gnns/aiim2023-baselines

Declaration of competing interest

None.

Acknowledgment

The work is a result of the project "Data-driven drug repositioning applying graph neural networks (3DR-GNN)", that is being developed under grant "PID2021-122659OB-I00" from the Spanish Ministerio de Ciencia e Innovación. This work has been supported by project MadridDataSpace4Pandemics, funded by Comunidad de Madrid (Consejería de Educación, Universidades, Ciencia y Portavocía) with FEDER funds as part of the response from the European Union to COVID-19 pandemic.

Appendix A. Supplementary data

Supplementary data to this article can be found online at https://doi.org/10.1016/j.artmed.2023.102687.

References

[1] Pushpakom S, et al. Drug repurposing: progress, challenges and recommendations. Nat Rev Drug Discov Jan. 2019;18(1):41–58. https://doi.org/10.1038/nrd.2018.168.

[2] Rudrapal M, Khairnar SJ, Jadhav AG. Drug repurposing (DR): an emerging approach in drug discovery, drug repurposing-hypothesis, molecular aspects and therapeutic applications. London, United Kingdom: IntechOpen; 2020. https://doi.org/10.5772/intechopen.93193.

[3] Cheng L, Li J, Ju P, Peng J, Wang Y. SemFunSim: a new method for measuring disease similarity by integrating semantic and gene functional association. PloS One Jun. 2014;9(6):e99415. https://doi.org/10.1371/journal.pone.0099415.

[4] Gysi DM, et al. Network medicine framework for identifying drug-repurposing opportunities for COVID-19. Proc Natl Acad Sci May 2021;118(19). https://doi.org/10.1073/pnas.2025581118.

[5] Hsieh K, et al. Drug repurposing for COVID-19 using graph neural network and harmonizing multiple evidence. Sci Rep Nov. 2021;11(1):1. https://doi.org/10.1038/s41598-021-02353-5.

[6] Doshi S, Chepuri SP. A computational approach to drug repurposing using graph neural networks. Comput Biol Med Nov. 2022;150:105992. https://doi.org/10.1016/j.compbiomed.2022.105992.

[7] Sosa DN, Derry A, Guo M, Wei E, Brinton C, Altman RB. A literature-based knowledge graph embedding method for identifying drug repurposing opportunities in rare diseases. Pac Symp Biocomput Pac Symp Biocomput 2020;25:463–74.

[8] Bajaj P, Heereguppe S, Sumanth C. Graph convolutional networks to explore drug and disease relationships in biological networks. Accessed: May 02, 2022. [Online]. Available: http://snap.stanford.edu/class/cs224w-2017/projects/cs224w-41-final.pdf; 2017.

[9] Prieto Santamaría L, Ugarte Carro E, Díaz Uzquiano M, Menasalvas Ruiz E, Pérez Gallardo Y, Rodríguez-González A. A data-driven methodology towards evaluating the potential of drug repurposing hypotheses. Comput Struct Biotechnol J Jan. 2021;19:4559–73. https://doi.org/10.1016/j.csbj.2021.08.003.

[10] Prieto Santamaría L, Díaz Uzquiano M, Ugarte Carro E, Ortiz-Roldán N, Pérez Gallardo Y, Rodríguez-González A. Integrating heterogeneous data to facilitate COVID-19 drug repurposing. Drug Discov Today Feb. 2022;27(2):558–66. https://doi.org/10.1016/j.drudis.2021.10.002.

[11] Barabási A-L, Gulbahce N, Loscalzo J. Network medicine: a network-based approach to human disease. Nat Rev Genet Jan. 2011;12(1):56–68. https://doi.org/10.1038/nrg2918.

[12] Žitnik M, Janjić V, Larminie C, Zupan B, Pržulj N. Discovering disease-disease associations by fusing systems-level molecular data. Sci Rep Nov. 2013;3. https://doi.org/10.1038/srep03202.

[13] Zhang Z, Cui P, Zhu W. Deep learning on graphs: a survey. IEEE Trans Knowl Data Eng 2020;34(1):249–70. https://doi.org/10.1109/TKDE.2020.2981333.

[14] Gaudelet T, et al. Utilizing graph machine learning within drug discovery and development. Brief Bioinform May 2021;(bbab159). https://doi.org/10.1093/bib/bbab159.

[15] Zhou J, et al. Graph neural networks: a review of methods and applications. AI Open Jan. 2020;1:57–81. https://doi.org/10.1016/j.aiopen.2021.01.001.

[16] Li MM, Huang K, Zitnik M. Graph representation learning in biomedicine and healthcare. Nat Biomed Eng Dec. 2022;6(12):12. https://doi.org/10.1038/s41551-022-00942-x.

[17] Abbas K, et al. Application of network link prediction in drug discovery. BMC Bioinformatics Apr. 2021;22(1):187. https://doi.org/10.1186/s12859-021-04082-y.

[18] A. Ayuso Muñoz et al., "REDIRECTION: Generating drug repurposing hypotheses using link prediction with DISNET data," in 2022 IEEE 35th international symposium on computer-based medical systems (CBMS).

[19] Lagunes-García G, Rodríguez-González A, Prieto-Santamaría L, del Valle EPG, Zanin M, Menasalvas-Ruiz E. DISNET: a framework for extracting phenotypic disease information from public sources. PeerJ Feb. 2020;8:e8580. https://doi.org/10.7717/peerj.8580.

[20] Goh K-I, Cusick ME, Valle D, Childs B, Vidal M, Barabási A-L. The human disease network. Proc Natl Acad Sci May 2007;104(21):8685–90. https://doi.org/10.1073/pnas.0701361104.

[21] Zhao B-W, et al. Fusing higher and lower-order biological information for drug repositioning via graph representation learning. IEEE Trans Emerg Top Comput 2023:1–14. https://doi.org/10.1109/TETC.2023.3239949.

[22] Su X, Hu P, Yi H, You Z, Hu L. Predicting drug-target interactions over heterogeneous information network. IEEE J Biomed Health Inform Jan. 2023;27(1):562–72. https://doi.org/10.1109/JBHI.2022.3219213.

[23] Zhong Y, et al. DDI-GCN: drug-drug interaction prediction via explainable graph convolutional networks. Artif Intell Med Oct. 2023;144:102640. https://doi.org/10.1016/j.artmed.2023.102640.

[24] LeCun Y, Bengio Y. Convolutional networks for images, speech, and time series. Handb Brain Theory Neural Netw 1995;3361(10):1995.

[25] Sperduti A, Starita A. Supervised neural networks for the classification of structures. IEEE Trans Neural Netw 1997;8(3):714–35. https://doi.org/10.1109/72.572108.

[26] Frasconi P, Gori M, Sperduti A. A general framework for adaptive processing of data structures. IEEE Trans Neural Netw 1998;9(5):768–86. https://doi.org/10.1109/72.712151.

[27] Bronstein MM, Bruna J, LeCun Y, Szlam A, Vandergheynst P. Geometric deep learning: going beyond Euclidean data. IEEE Signal Process Mag Jul. 2017;34(4):18–42. https://doi.org/10.1109/MSP.2017.2693418.

[28] Perozzi B, Al-Rfou R, Skiena S. DeepWalk: online learning of social representations. In: Proceedings of the 20th ACM SIGKDD international conference on knowledge discovery and data mining, in KDD '14. New York, NY, USA: Association for Computing Machinery; Aug. 2014. p. 701–10. https://doi.org/10.1145/2623330.2623732.

[29] Grover A, Leskovec J. node2vec: Scalable feature learning for networks. In: Proceedings of the 22nd ACM SIGKDD international conference on knowledge discovery and data mining, in KDD '16. New York, NY, USA: Association for Computing Machinery; Aug. 2016. p. 855–64. https://doi.org/10.1145/2939672.2939754.

[30] Hamilton WL. Graph representation learning. Synth Lect Artif Intell Mach Learn Sep. 2020;14(3):1–159. https://doi.org/10.2200/S01045ED1V01Y202009AIM046.

[31] Zhou Y, Hou Y, Shen J, Huang Y, Martin W, Cheng F. Network-based drug repurposing for novel coronavirus 2019-nCoV/SARS-CoV-2. Cell Discov Mar. 2020;6(1):1–18. https://doi.org/10.1038/s41421-020-0153-3.

[32] Zeng X, et al. Repurpose open data to discover therapeutics for COVID-19 using deep learning. J Proteome Res Nov. 2020;19(11):4624–36. https://doi.org/10.1021/acs.jproteome.0c00316.
[33] Ioannidis VN, Zheng D, Karypis G. Few-shot link prediction via graph neural networks for Covid-19 drug-repurposing. ArXiv200710261 Cs Stat Jul. 2020. Accessed: Nov. 16, 2021. [Online]. Available: http://arxiv.org/abs/2007.10261.
[34] Drug Repurposing Knowledge Graph (DRKG). gnn4dr 2020. Accessed: Feb. 20, 2023. [Online]. Available: https://github.com/gnn4dr/DRKG.
[35] Mei X, Cai X, Yang L, Wang N. Relation-aware heterogeneous graph transformer based drug repurposing. Expert Syst Appl Mar. 2022;190:116165. https://doi.org/10.1016/j.eswa.2021.116165.
[36] Gu Y, Zheng S, Yin Q, Jiang R, Li J. REDDA: integrating multiple biological relations to heterogeneous graph neural network for drug-disease association prediction. Comput Biol Med Nov. 2022;150:106127. https://doi.org/10.1016/j.compbiomed.2022.106127.
[37] The comparative toxicogenomics database | CTD. Accessed: Jan. 11, 2022. [Online]. Available: http://ctdbase.org/.
[38] Zitnik M, Agrawal M, Leskovec J. Modeling polypharmacy side effects with graph convolutional networks. Bioinforma Oxf Engl Jul. 2018;34(13):i457–66. https://doi.org/10.1093/bioinformatics/bty294.
[39] Percha B, Altman RB. A global network of biomedical relationships derived from text. Bioinforma. Oxf. Engl. Aug. 2018;34(15):2614–24. https://doi.org/10.1093/bioinformatics/bty114.
[40] Brown AS, Patel CJ. A standard database for drug repositioning. Sci Data Mar. 2017;4(1):170029. https://doi.org/10.1038/sdata.2017.29.
[41] Hamilton W, Ying Z, Leskovec J. Inductive representation learning on large graphs. In: Advances in Neural Information Processing Systems. Curran Associates, Inc.; 2017. Accessed: Nov. 04, 2021. [Online]. Available: https://proceedings.neurips.cc/paper/2017/hash/5dd9db5e033da9c6fb5ba83c7a7ebea9-Abstract.html.
[42] Mikolov T, Sutskever I, Chen K, Corrado GS, Dean J. Distributed representations of words and phrases and their compositionality. In: Advances in neural information processing systems. Curran Associates, Inc.; 2013. Accessed: May 09, 2022. [Online]. Available: https://papers.nips.cc/paper/2013/hash/9aa42b31882ec039965f3c4923ce901b-Abstract.html.
[43] Trouillon T, Welbl J, Riedel S, Gaussier E, Bouchard G. Complex embeddings for simple link prediction. In: Proceedings of the 33rd international conference on machine learning. PMLR; Jun. 2016. p. 2071–80. Accessed: May 09, 2022. [Online]. Available: https://proceedings.mlr.press/v48/trouillon16.html.
[44] Biewald L. Experiment tracking with weights and biases [Online]. Available: https://www.wandb.com/; 2020.
[45] Mikolov T, Chen K, Corrado G, Dean J. Efficient estimation of word representations in vector space. arXiv 2013. https://doi.org/10.48550/arXiv.1301.3781. Sep. 06.
[46] Qiu J, Dong Y, Ma H, Li J, Wang K, Tang J. Network embedding as matrix factorization: unifying DeepWalk, LINE, PTE, and node2vec. In: Proceedings of the eleventh ACM international conference on web search and data mining. Marina Del Rey CA USA: ACM; Feb. 2018. p. 459–67. https://doi.org/10.1145/3159652.3159706.
[47] Ahmed NK, et al. Learning role-based graph embeddings. arXiv 2018. https://doi.org/10.48550/arXiv.1802.02896. Jul. 02.
[48] Rozemberczki B, Kiss O, Sarkar R. Karate Club: an API oriented open-source Python framework for unsupervised learning on graphs. In: Proceedings of the 29th ACM International Conference on Information & Knowledge Management, CIKM '20. New York, NY, USA: Association for Computing Machinery; 2020. p. 3125–32. https://doi.org/10.1145/3340531.3412757.
[49] Spackman KA. Signal detection theory: valuable tools for evaluating inductive learning. In: Segre AM, editor. Proceedings of the sixth international workshop on machine learning. San Francisco (CA): Morgan Kaufmann; 1989. p. 160–3. https://doi.org/10.1016/B978-1-55860-036-2.50047-3.
[50] Davis J, Goadrich M. The relationship between precision-recall and ROC curves. presented at the Proceedings of the 23rd International Conference on Machine Learning. ACM; Jun. 2006. https://doi.org/10.1145/1143844.1143874.
[51] Kim J-H. Estimating classification error rate: repeated cross-validation, repeated hold-out and bootstrap. Comput Stat Data Anal Sep. 2009;53(11):3735–45. https://doi.org/10.1016/j.csda.2009.04.009.
[52] Schocken DD, Arrieta MI, Leaverton PE, Ross EA. Prevalence and mortality rate of congestive heart failure in the United States. J Am Coll Cardiol Aug. 1992;20(2):301–6. https://doi.org/10.1016/0735-1097(92)90094-4.
[53] Rengo F, et al. Congestive heart failure in the elderly. Arch Gerontol Geriatr Nov. 1996;23(3):201–23. https://doi.org/10.1016/S0167-4943(96)00734-0.
[54] Keating GM, Goa KL. Nesiritide. Drugs Jan. 2003;63(1):47–70. https://doi.org/10.2165/00003495-200363010-00004.
[55] Colucci WS. Nesiritide for the treatment of decompensated heart failure. J Card Fail Mar. 2001;7(1):92–100. https://doi.org/10.1054/jcaf.2001.22999.
[56] Mahle WT, Cuadrado AR, Kirshbom PM, Kanter KR, Simsic JM. Nesiritide in infants and children with congestive heart failure. Pediatr Crit Care Med J Soc Crit Care Med World Fed Pediatr Intensive Crit Care Soc Sep. 2005;6(5):543–6. https://doi.org/10.1097/01.pcc.0000164634.58297.9a.
[57] Malm-Erjefält M, et al. Metabolism and excretion of the once-daily human glucagon-like peptide-1 analog liraglutide in healthy male subjects and its in vitro degradation by dipeptidyl peptidase IV and neutral endopeptidase. Drug Metab Dispos Biol Fate Chem Nov. 2010;38(11):1944–53. https://doi.org/10.1124/dmd.110.034066.
[58] Russell-Jones D. Molecular, pharmacological and clinical aspects of liraglutide, a once-daily human GLP-1 analogue. Mol Cell Endocrinol Jan. 2009;297(1):137–40. https://doi.org/10.1016/j.mce.2008.11.018.
[59] Arturi F, et al. Liraglutide improves cardiac function in patients with type 2 diabetes and chronic heart failure. Endocrine Sep. 2017;57(3):464–73. https://doi.org/10.1007/s12020-016-1166-4.
[60] Scott DL, Wolfe F, Huizinga TW. Rheumatoid arthritis. Lancet Sep. 2010;376(9746):1094–108. https://doi.org/10.1016/S0140-6736(10)60826-4.
[61] Littlejohn EA, Monrad SU. Early diagnosis and treatment of rheumatoid arthritis. Prim Care Clin Off Pract Jun. 2018;45(2):237–55. https://doi.org/10.1016/j.pop.2018.02.010.
[62] Hewitson, DeBroe, McBride, Milne. Leflunomide and rheumatoid arthritis: a systematic review of effectiveness, safety and cost implications. J Clin Pharm Ther 2000;25(4):295–302. https://doi.org/10.1046/j.1365-2710.2000.00296.x.
[63] Sanders S, Harisdangkul V. Leflunomide for the treatment of rheumatoid arthritis and autoimmunity. Am J Med Sci Apr. 2002;323(4):190–3. https://doi.org/10.1097/00000441-200204000-00004.
[64] Behrens F, Koehm M, Burkhardt H. Update 2011: leflunomide in rheumatoid arthritis – strengths and weaknesses. Curr Opin Rheumatol May 2011;23(3):282. https://doi.org/10.1097/BOR.0b013e328344fddb.
[65] Williamson RA, et al. Dihydroorotate dehydrogenase is a target for the biological effects of leflunomide. Transplant Proc Dec. 1996;28(6):3088–91.
[66] Breedveld FC, Dayer J-M. Leflunomide: mode of action in the treatment of rheumatoid arthritis. Ann Rheum Dis Nov. 2000;59(11):841–9. https://doi.org/10.1136/ard.59.11.841.
[67] Fox RI, et al. Mechanism of action for Leflunomide in rheumatoid arthritis. Clin Immunol Dec. 1999;93(3):198–208. https://doi.org/10.1006/clim.1999.4777.
[68] Ajayi S, et al. Ruxolitinib. In: Martens UM, editor. Small molecules in hematology. Recent Results in Cancer Research. Cham: Springer International Publishing; 2018. p. 119–32. https://doi.org/10.1007/978-3-319-91439-8_6.
[69] McLornan DP, Pope JE, Gotlib J, Harrison CN. Current and future status of JAK inhibitors. The Lancet Aug. 2021;398(10302):803–16. https://doi.org/10.1016/S0140-6736(21)00438-4.
[70] Igaz P, Tóth S, Falus A. Biological and clinical significance of the JAK-STAT pathway; lessons from knockout mice. Inflamm Res Sep. 2001;50(9):435–41. https://doi.org/10.1007/PL00000267.
[71] McLornan DP, Khan AA, Harrison CN. Immunological consequences of JAK inhibition: friend or foe? Curr Hematol Malig Rep Dec. 2015;10(4):370–9. https://doi.org/10.1007/s11899-015-0284-z.
[72] Baldini C, Moriconi FR, Galimberti S, Libby P, De Caterina R. The JAK–STAT pathway: an emerging target for cardiovascular disease in rheumatoid arthritis and myeloproliferative neoplasms. Eur Heart J Nov. 2021;42(42):4389–400. https://doi.org/10.1093/eurheartj/ehab447.
[73] Yamaoka K. Janus kinase inhibitors for rheumatoid arthritis. Curr Opin Chem Biol Jun. 2016;32:29–33. https://doi.org/10.1016/j.cbpa.2016.03.006.
[74] Baker KF, Isaacs JD. Novel therapies for immune-mediated inflammatory diseases: what can we learn from their use in rheumatoid arthritis, spondyloarthritis, systemic lupus erythematosus, psoriasis, Crohn's disease and ulcerative colitis? Ann Rheum Dis Feb. 2018;77(2):175–87. https://doi.org/10.1136/annrheumdis-2017-211555.
[75] Angelini J, et al. JAK-inhibitors for the treatment of rheumatoid arthritis: a focus on the present and an outlook on the future. Biomolecules Jul. 2020;10(7):7. https://doi.org/10.3390/biom10071002.
[76] Cuspidi C, Sala C, Negri F, Mancia G, Morganti A. Prevalence of left-ventricular hypertrophy in hypertension: an updated review of echocardiographic studies. J Hum Hypertens Jun. 2012;26(6):6. https://doi.org/10.1038/jhh.2011.104.
[77] Díez J, Frohlich ED. A translational approach to hypertensive heart disease. Hypertension Jan. 2010;55(1):1–8. https://doi.org/10.1161/HYPERTENSIONAHA.109.141887.
[78] Nwabuo CC, Vasan RS. Pathophysiology of hypertensive heart disease: beyond left ventricular hypertrophy. Curr Hypertens Rep Feb. 2020;22(2):11. https://doi.org/10.1007/s11906-020-1017-9.
[79] Singh JSS, Burrell LM, Cherif M, Squire IB, Clark AL, Lang CC. Sacubitril/valsartan: beyond natriuretic peptides. Heart Oct. 2017;103(20):1569–77. https://doi.org/10.1136/heartjnl-2017-311295.
[80] Imamura T, Kinugawa K. Effect of add-on sacubitril/valsartan on the left ventricular hypertrophy of a patient with hypertension. J Int Med Res Nov. 2022;50(11). https://doi.org/10.1177/03000605221138480. p. 03000605221138480.
[81] Singh JS, Lang CC. Angiotensin receptor-neprilysin inhibitors: clinical potential in heart failure and beyond. Vasc Health Risk Manag Jun. 2015;11:283–95. https://doi.org/10.2147/VHRM.S55630.
[82] Cohn JN, Tognoni G. A randomized trial of the angiotensin-receptor blocker valsartan in chronic heart failure. N Engl J Med Dec. 2001;345(23):1667–75. https://doi.org/10.1056/NEJMoa010713.